International Journal of Thermophysics, Vol. 22, No. 2, 2001

NMR Study of Chain Motion in Atactic Polypropylene at High Pressure[1]

A. G. S. Hollander[2] and K. O. Prins[2, 3]

Deuteron solid-state NMR techniques at high pressure are used to study the chain dynamics in the amorphous polymer atactic polypropylene. The arrest of the structural relaxation above the glass-transition temperature T_g is investigated using one- and two-dimensional deuteron NMR spectra. The slow reorientation of the main chain segments is identified with the α-process observed in mechanical relaxation experiments. On approaching the glass transition, the time scale of the collective motion of the main chain becomes longer very rapidly at decreasing temperatures. Along isobars, at pressure values up to 5 kbar, the temperature dependence of the logarithmic average correlation time is very well described by a Vogel–Fulcher function. The motion of the main chain is strongly dependent on the pressure, while its character is determined mainly by the distance to T_g. The introduction of the equation of state allows the investigation of the dynamic behavior on isothermal and isochoric paths on approaching T_g. It is found that along an isotherm the mobility as a function of the density is also of the Vogel–Fulcher form.

KEY WORDS: atactic polypropylene; glass transition; high pressure; NMR; slow chain motion.

1. INTRODUCTION

The arrest of the structural relaxation at the glass transition is an important aspect of polymer glasses. At temperatures just above the glass transition the diffusive motion and the conformational changes of the main chain (the α-process) slow down drastically. In amorphous polymers its temperature dependence is very well described by the Williams–Landel–Ferry

[1] Invited paper presented at the Fourteenth Symposium on Thermophysical Properties, June 25–30, 2000, Boulder, Colorado, U.S.A.

[2] Van der Waals-Zeeman Institute, University of Amsterdam, Valckenierstraat 65, 1018 XE Amsterdam, The Netherlands.

[3] To whom correspondence should be addressed. E-mail: kprins@wins.uva.nl

0195-928X/01/0300-0357$19.50/0

(WLF) equation [1, 2] or, equivalently, by the Vogel–Fulcher–Tammann–Hesse function [3–5]. The time scale of the structural relaxation changes over about 15 orders of magnitude. The large change in the mechanical properties at the glass transition is related to the change in the molecular dynamics.

In this paper we present a study of the effect of high pressure on the chain dynamics of atactic polypropylene (aPP) in the liquid close to the glass transition. This study is an extension to conditions of high pressure of the work in deuterated aPP by Spiess and co-workers [6, 7] at ambient pressure with the technique of two-dimensional (2D) exchange deuteron NMR. They found that the spectra obtained could be successfully reproduced by assuming isotropic rotational diffusion asthe model for the slow reorientation of the main chain segments. All data obtained from these experiments, combined with those determined earlier through measurements of ^{13}C spin-lattice relaxation times [8] at elevated temperatures, could be represented quantitatively over more than 12 orders of magnitude by the WLF equation. The conclusion was that the time scales of the chain dynamics as probed for individual chain segments by 2D NMR are in excellent agreement with those of the collective processes responsible for the strong temperature dependence of the α-relaxation process.

In this study we first show that at high pressure, up to 5 kbar, the slowing-down of the main chain motion on approaching the glass transition can be represented very well by the WLF equation. Next, we introduce the equation of state to investigate the dynamic behavior on isothermal and isochoric paths, to separate the effects of the changes in temperature and in density on approaching the glass transition.

2. EXPERIMENTAL

We used a sample of 88% uniformly deuterated atactic polypropylene, prepared from the same material as used in Ref. 6. The molecular weight (by viscometry) is $M_w \approx 25{,}000\ \mathrm{g \cdot mol^{-1}}$. With differential scanning calorimetry the value of T_g of this deuterated aPP material was determined to be 253 K at ambient pressure.

The NMR spectrometer and high-pressure NMR probe used for the investigation presented in this paper have been described in detail elsewhere [9]. The experiments have been performed at a ^2H-NMR frequency of 41.433 MHz with $\pi/2$ radio frequency pulses of 4 μs.

We obtained one-dimensional (1D) quadrupole echo [10] spectra using the standard sequence of two radiofrequency pulses with a phase difference $\pi/2$, separated by a time interval τ_1. We obtained 2D exchange spectra by using the five-pulse sequence described in Ref. 11.

High-purity (at least 99.999%) helium gas is used as the pressurizing medium. Helium is used because of its very low solubility in hydrocarbon liquids and elastomers. The equipment for the generation and measurement of pressure has also been described in Ref. 9.

3. NMR SPECTRA

3.1. ^{2}H-NMR Quadrupole Echo Spectra

The interaction dominating the ^{2}H-NMR spectra in deuterated hydrocarbon polymers is the coupling between the electric quadrupole moment eQ of the deuteron (with spin quantum number $I=1$) and the electric field gradient (EFG) at the site of the deuteron. For a single C–D bond, the combined Zeeman and quadrupole Hamiltonians lead to a deuteron NMR spectrum consisting of only two lines, at frequencies

$$\omega = \omega_0 \pm \delta_Q(3\cos^2\theta - 1 + \eta\sin^2\theta\cos 2\varphi) = \omega_0 \pm \omega_Q(\theta, \varphi) \tag{1}$$

where ω_0 is the deuteron Zeeman frequency and $\delta_Q \equiv 3e^2qQ/(8h)$, while eq is the value of the principal value $\partial^2V/\partial z^2$ of the EFG tensor; η is the asymmetry parameter $(\partial^2V/\partial x^2 - \partial^2V/\partial y^2)/\partial^2V/\partial z^2$. The quadrupole frequency shift ω_Q depends on the polar angles θ and φ of the static magnetic field $\boldsymbol{B}$ in the principal axes system (PAS) of the EFG tensor. The much weaker magnetic dipole–dipole interactions, present in the system of nuclear spins, result in a homogeneous broadening (to a width of only about 1 kHz) of each line. In an aliphatic C–D bond, the EFG is nearly axially symmetric ($\eta = 0$) and the quadrupole constant e^2qQ/h is $(2\pi)169 \times 10^3$ rads^{-1}.

For an isotropic distribution of C–D bond orientations, such as present in a rigid amorphous deuterated-polymer solid, the quadrupole echo spectrum arising from the two transitions in Eq. (1) is the Pake doublet [12], with characteristic singularities at frequencies $\pm\delta_Q$ corresponding to $\theta = \pi/2$. Figure 1 shows the 1D deuteron quadrupole echo spectrum in the glassy state at ambient pressure at 246 K. As shown schematically, the spectrum consists of a superposition of two Pake doublets. The broad component, with a distance between the singularities Δ_{chain} of about 123 kHz, originates from deuterons directly bonded to the almost-immobile main chain. The distance is slightly smaller than the value 127 kHz expected from the value of the quadrupole coupling constant. This is due to restricted reorientation of the main chain C–D bonds, occurring on a time scale of 10^{-6} s, shorter than δ_Q^{-1}. The narrow component, with a distance between the singularities Δ_{methyl} of about 37 kHz, is the contribution from the deuterons of the methyl groups, which perform rapid anisotropic

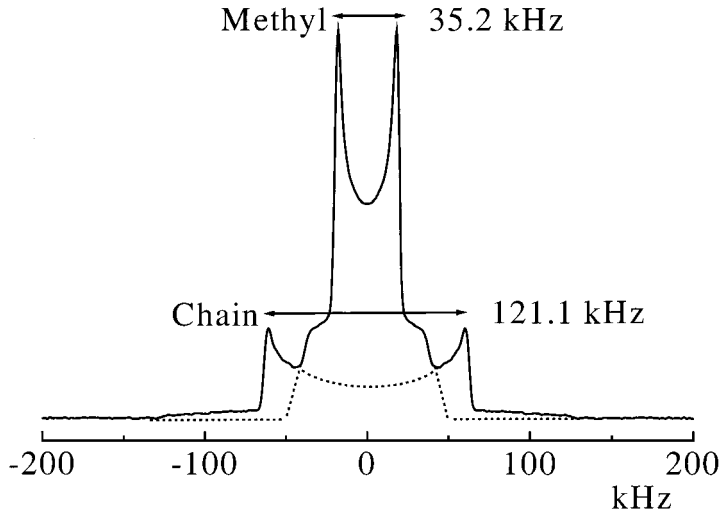

Fig. 1. Experimental quadrupole echo ^{2}H NMR spectrum of aPP in the glassy state at 246 K and 1 bar. The dotted lines indicate that it consists of two Pake doublets, originating from methyl and chain deuterons.

reorientation on a time scale of about 10^{-10} s, very much shorter than δ_Q^{-1}. As a result, the methyl deuterons experience an average EFG which is axial about the C_3 axis with $\overline{eq} = eq/3$ for a tetrahedral configuration of bonds.

3.2. ^{2}H 2D Exchange NMR Spectra

For the observation of the very slow motion occurring just above the glass-transition temperature, on a time scale of 10^{-5} to 10^2 s, we made use of the technique of deuteron 2D exchange NMR. Theory and application of this technique are comprehensively presented in the textbook by Schmidt-Rohr and Spiess [13]. As mentioned above, we obtained 2D exchange spectra by using the five-pulse sequence described in Ref. 11.

The 2D exchange absorption spectrum $S(\omega_1, \omega_2; t_m)$ may be identified with the joint probability density $P(\omega_1, \omega_2; t_m)$ that a nucleus has an NMR frequency ω_1 before and a frequency ω_2 after the "mixing" time t_m included in the pulse sequence. As discussed above, the ^{2}H-NMR frequency is a function of the orientation of the external magnetic field $\boldsymbol{B}$ with respect to the principal axis system of the EFG present at the site of the nucleus. Since in a C–^{2}H bond the EFG is approximately axially symmetric about the bond direction, one can map the frequency domain (ω_1, ω_2) onto the polar angle domain (θ_1, θ_2) and associate with $P(\omega_1, \omega_2; t_m)$ the joint probability density $P'(\theta_1, \theta_2; t_m)$ of finding the angles θ_1 and θ_2 between

the C–^{2}H bond and $\boldsymbol{B}$ before and after a time interval t_m, respectively. From this, one can construct the distribution $W(\xi, t_m)$ of the angle ξ of reorientation of the C–^{2}H bond after a time interval t_m. The angular information contained in a ^{2}H 2D exchange spectrum is completely specified by the 1D reorientation angle distribution $W(\xi, t_m)$. By systematically varying t_m, one is able to monitor the dynamic evolution of $P(\omega_1, \omega_2; t_m)$ and of $W(\xi; t_m)$, and to determine the type and time scale of the molecular reorientation.

The above is strictly true only in the so-called slow-motion limit, in which a C–^{2}H bond reorients only during t_m, and not in t_1 or in t_2. The interpretation given is therefore valid in practice only for motion with a characteristic time longer than 10^{-3} s. In the intermediate exchange regime (10^{-5} to 10^{-3} s), the correspondence between the 2D exchange spectrum $S(\omega_1, \omega_2; t_m)$ and the joint probability density $P(\omega_1, \omega_2; t_m)$ breaks down. However, by incorporating the effect of motion on an intermediate time scale on the calculated 2D spectra [7, 14], the dynamic range, for which experimental and calculated spectra can be compared and reorientation angle distributions $W(\xi; t_m)$ are obtained, is extended from 10^{-3} to 10^{-5} s.

Figure 2 shows a typical ^{2}H 2D exchange spectrum $S(\omega_1, \omega_2; t_m)$ of aPP. It was determined at 973 bar and at 284 K, which is 17 K above T_g at that pressure. The mixing time $t_m = 50$ ms. The spectrum appears to be very similar to the one shown in Ref. 6, determined at ambient pressure at 270 K, which is also 17 K above T_g.

Along the $\omega_1 = \omega_2$ diagonal we recognize the shape of the 1D ^{2}H spectrum in Fig. 1, namely, a superposition of the two Pake patterns originating from the chain and the methyl deuterons. The intensity of the spectrum along the diagonal represents C–^{2}H bonds, which, after 50 ms, are found to have the same angle with respect to the magnetic field $\boldsymbol{B}$ as at the start of the experiment. The off-diagonal intensity, in particular the ridges parallel to the singularities in ω_1 and in ω_2, indicates reorientation motion occurring at the time scale of the mixing time. The reorientation of the main chain segments causes exchange within both the chain and the methyl deuteron frequencies. The exchange is visible covering all frequencies within two square-like areas. This can be understood as a superposition of 2D spectra according to a distribution of reorientation angles. The ridges $S(\pm\delta_Q, \omega_2)$ at $\omega_1 = \pm\delta_Q = \pm 18$ kHz (the peaks of the methyl Pake pattern) correspond to C–C^{2}H$_3$ bonds that have an orientation perpendicular to $\boldsymbol{B}$ at the start of the mixing period. From these ridges it can already be seen that the reorientation angle distribution $W(\xi; t_m)$ is a continuous distribution, indicating that after 50 ms the axis of the methyl group has a finite probability to be found in any orientation with respect to the magnetic field, regardless of its starting position. Reorientation over discrete and fixed

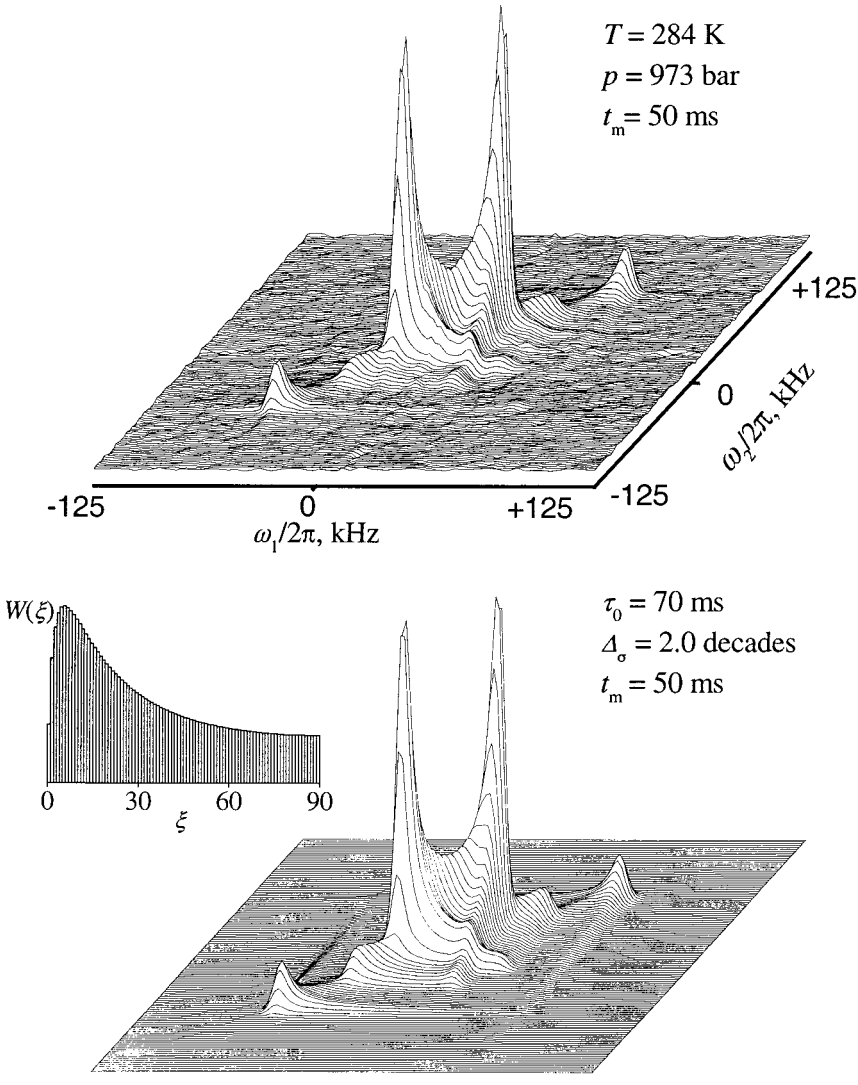

Fig. 2. Typical ^{2}H 2D exchange spectrum of aPP. (a) Experiment at 973 bar and 284 K with a mixing time $t_m = 50$ ms. (b) Calculated spectrum, with the same frequency scales as the experimental spectrum, with $\tau_0 = 70$ ms and $\Delta_\sigma = 2$ decades. The inset shows the corresponding reorientation angle distribution $W(\xi)$.

angles would cause typical elliptical ridge pattern [13, 15]. These are not visible in our spectra of aPP.

We performed ^{2}H 2D exchange NMR experiments along isobars at 1, 973, 1978, and 4986 bar, in temperature ranges from about 11 to about 34 K above T_g. At each temperature and pressure value, we obtained two 2D absorption spectra by choosing two mixing times t_m, with a ratio of 3 to 10. At the lower end of each temperature range the correlation time becomes much longer than the mixing time, allowed by the spin-lattice relaxation time.

We used the values of T_g at each pressure value as they have been obtained from the decay of the quadrupole echo in Ref. 9, where the data could be represented by the quadratic function

$$p(T_g) = b_1(T_g - T_g^0) + b_2(T_g - T_g^0)^2 \tag{2}$$

in which T_g^0 is the glass-transition temperature at zero pressure, with the following values of the parameters: $b_1 = 55(\pm 12)$ bar $\cdot$ K^{-1}, $b_2 = 0.48(\pm 0.16)$ bar $\cdot$ K^{-2}, and $T_g^0 = 251.2(\pm 2.1)$ K.

4. MODEL FOR THE CHAIN REORIENTATION

In the analysis of the 2D exchange spectra we assume that in aPP the reorientation motion of the chain segments above the glass transition temperature results in isotropic rotational diffusion of the directions of both the main chain C–^{2}H bonds and the C–C^{2}H$_3$ bonds, with the same diffusion coefficient D_r. This process can also be characterized by a correlation time $\tau_d = 1/6D_r$. Spiess and co-workers have shown [Ref. 16, Eqs. (6) and (10)] that, essentially, the 2D absorption spectrum $S(\omega_1, \omega_2; t_m)$ can be derived from the rotational diffusion equation.

The characterization of the time scale of the motion requires the introduction of a distribution of correlation times. This is immediately clear, for instance, in the experimental spectrum at 1 bar and 284 K in Fig. 3, where a narrow peak indicating fast quasi-isotropic motion occurs in the center, together with the effects of exchange on a much slower time scale.

The occurrence of a correlation time distribution is related to the non-exponential loss of correlation in the chain relaxation process [17], following the Kohlrausch–Williams–Watts (KWW) relaxation function [18, 19] $C(t) = \exp[-(t/t_{KWW})^\beta]$. The correlation time distribution, obtained as the Laplace transform of the KWW function, resembles a Gaussian distribution of $\ln \tau_d$ values, apart from showing a more rapid decrease in the wing at long τ_d values.

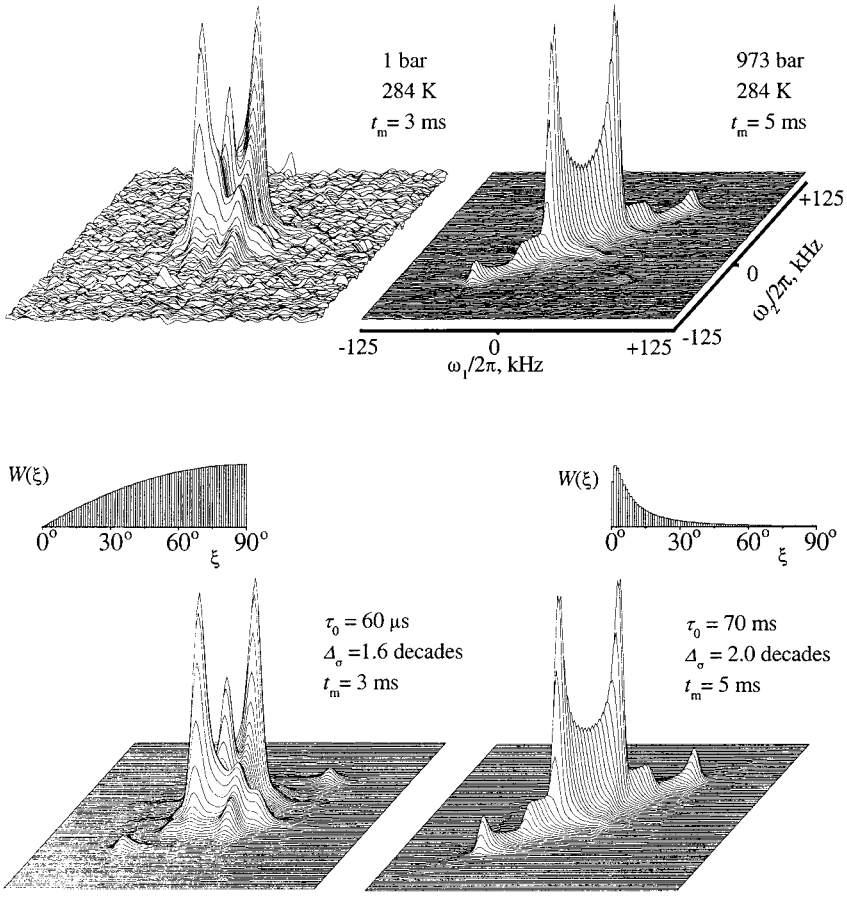

Fig. 3. ^{2}H 2D exchange spectra as a function of pressure. The experiments were performed at 1 bar and 284 K and at 973 bar and 284 K with mixing times $t_m = 3$ and 5 ms, respectively.

Although it is possible, in principle, to make the data analysis by using correlation time distributions, obtained as Laplace transforms of KWW functions with varying τ_{KWW} and β values, we choose the simpler approach of using a Gaussian distribution of $\ln \tau_d$ values:

$$\rho(\ln \tau_d) = \frac{1}{\sigma\sqrt{2\pi}} \exp\left\{-\frac{(\ln \tau_d - \ln \tau_0)^2}{2\sigma^2}\right\} \tag{3}$$

where $\ln \tau_0$ is the mean value of $\ln \tau_d$ and σ is the standard deviation of the distribution. The width Δ_σ of the distribution expressed in decades is $2\sigma^{10}\log(e)$.

4.1. Calculation of Spectra

We compared the experimental spectra with spectra calculated using a computer program based on the analysis as presented in Refs. 7, 14, 16, and 20. Two-dimensional time domain responses generated by a five-pulse sequence are calculated, using rotational diffusion as the model for the chain segment reorientation. This calculation is performed separately for the chain deuterons and for the methyl deuterons, using axially symmetric EFG tensors. We account for the effect of the fast small-angle reorientation, resulting in the reduced distance of the Pake singularities in the 1D spectra, by using reduced quadrupole coupling constants $(2\pi)161.6 \times 10^3$ and $(2\pi)48.3 \times 10^3$ rad $\cdot$ s^{-1} for the chain deuterons and the methyl deuterons, respectively. In this way the Pake singularities in the calculated spectra appear at the frequencies of the maxima in the experimental spectra.

As shown in Fig. 2, the experimental spectrum at 973 bar and 284 K obtained with $t_m = 50$ ms can be reproduced very well by choosing a correlation time distribution with $\tau_0 = 70$ ms and $\Delta_\sigma = 2$ decades. Also shown is the reorientation angle distribution $W(\xi)$ corresponding to this distribution of τ_d. Another experiment with $t_m = 5$ ms was performed at the same temperature and pressure (see Fig. 3), and an excellent fit was obtained using a distribution with precisely the same parameters.

A clear example of the effect of pressure on the dynamics is shown in Fig. 3. Here we compare two spectra at 284 K, at 1 bar and at 973 bar. The experiments have been performed with approximately equal mixing times, namely, $t_m = 3$ and 5 ms, respectively. At 1 bar a lot of exchange intensity is visible, as is the peak in the center of the spectrum due to nearly isotropic motion, indicating that a substantial part of the main chain segments are reorienting with correlation times $\tau_d \leqslant 1\ \mu$s. After an increase in the pressure to about 1 kbar, the exchange intensity almost disappears. This can also be seen from the reorientation angle distributions and the correlation time distributions, as obtained from fitting calculated spectra to the experimental spectra. The logarithmic average correlation time τ_0 decreases three orders of magnitude on increasing the pressure to about 1 kbar.

The use of 2D exchange NMR to observe molecular reorientation is possible only within a limited temperature range. At the lowest temperature the spin-lattice relaxation time limits the mixing time, and, in the case of aPP, a correlation time τ_d longer than approximately 100 s cannot be observed. At high temperatures the spectrum collapses into an isotropic peak for $\tau_d \approx 1\ \mu$s. In practice, this means that for $\tau_0 \leqslant 50\ \mu$s, for aPP corresponding to temperatures $T \geqslant T_g + 35$ K, information about the molecular reorientation cannot be obtained any more from 2D exchange spectra.

Of course, the motion of the chain segments cannot truly be isotropic, because of the restrictions imposed on the chain segments by the polymer main chain itself and by its environment. We note that the quadrupole coupling Hamiltonian possesses inversion symmetry; reorientation angles ξ cannot be distinguished from angles $\pi - \xi$. Therefore, quasi-isotropic motion of the chain segments will still result in the same line shapes as produced by isotropic motion.

It must be noted that, as a 2D exchange spectrum correlates the orientations of C–^{2}H bonds only before and after a time period t_m, the effect on the reorientation angle distribution $W(\xi; t_m)$ produced by another isotropic reorientation process, but much slower than the rotational diffusion, is not detectable. Hence, its possible existence cannot be excluded. To detect other, slower, motional processes, the use of three- or higher-dimensional NMR techniques would be necessary.

5. 1D ^{2}H-NMR SPECTRA

To observe faster chain motion, on a time scale of 10^{-4} to 10^{-6} s, occurring at higher temperatures we obtained information from 1D ^{2}H-NMR quadrupole echo spectra, namely, at 1 bar (where $T_g = 250$ K) in the temperature range 280 to 315 K and at 4986 bar (where $T_g = 311$ K) for 348 and 353 K. Figure 4 shows some quadrupole echo spectra as a function of the pulse distance τ_1. Clearly, in this temperature range the line shape shows a strong dependence on the time scale of the molecular motion.

The effect of molecular motion on the line shape in quadrupole echo spectra can be described with a multisite exchange formalism [21], which follows Abragam's treatment of motion narrowing [23]. With the help of a computer program, based on this formalism and kindly provided by the late Prof. Dr. Regitze Vold, we calculate the quadrupole echo spectrum resulting from the C–^{2}H bond jumping between N discrete orientations, using as a parameter the mean time τ_j between jumps. To simulate the isotropic diffusive nature of the reorientation, we mimic it by an isotropic random walk on a sphere, while the orientations of a C–^{2}H bond are limited to the orientations of the position vectors from the center to the carbon atoms in a C_{60} molecule. From every orientation, only jumps to the three nearest neighbors are allowed. We again used the log-normal distribution, Eq. (1), for τ_j. Some of the results are shown in Fig. 4.

As can be seen, the discrete jump model results in satisfactory fits to spectra obtained at temperatures $T = 284$ K and higher. The calculations do not yield acceptable fits to the spectra at lower temperatures. Presumably, this is due to the crudeness of the model; it breaks down when

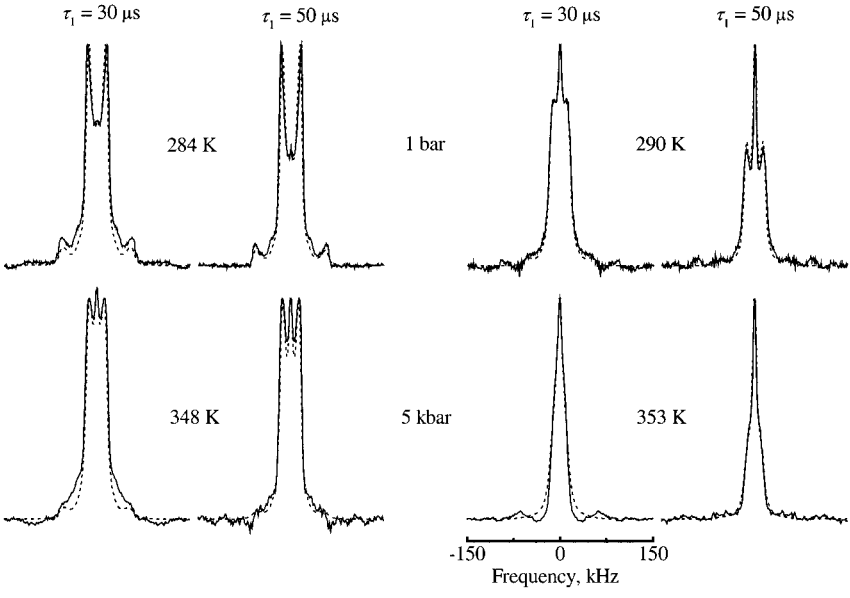

Fig. 4. Experimental quadrupole echo spectra at 284 and 290 K at 1 bar and at 348 and at 353 K at 4986 bar and the corresponding calculated spectra obtained from the discrete model (see text), as a function of the pulse distance.

the correlation times become long and the reorientation angles become of the size corresponding to one jump in the discrete model. As in the calculations of the 2D spectra, the choice of asymmetric distributions does not result in substantially better fits.

To relate τ_j with τ_d, and therefore τ_{j0} with τ_0, we have calculated the distribution $W(\xi; t)$ of the relative reorientation angle ξ of a C–^{2}H bond after a time t, both for the discrete model as described above and for isotropic diffusion, for which an analytical expression has been derived from the solution of the rotation diffusion equation (as presented in, e.g., Ref. 22). From the comparison it appears that $\tau_d \approx 4.5\tau_j$. The distributions of τ_j are converted to distributions of τ_d accordingly.

Information on still faster motion, on a time scale of 10^{-6} to 10^{-8} s, was derived from motional narrowed spectra [23], obtained from free induction decays following a single $\pi/2$ pulse. Above about $T_g + 50$ K the motion of the C–^{2}H bonds becomes sufficiently isotropic and rapid to average the EFG to zero, and the quadrupole echo pulse sequence fails to create a quadrupole echo. The experimental line shapes obtained at temperature values from $T_g + 50$ to $T_g + 83$ K (at ambient pressure only) are found to be non-Lorentzian. For isotropic reorientation with a single value

of the correlation τ_d, there is a simple relation [23] between the transverse relaxation rate $1/T_2$ and τ_d. Calculated line shapes are obtained by adding the Lorentzian line shapes, corresponding to values of τ_d, and weighted again according to a log-normal distribution. In this way, good fits to the experimental spectra are obtained.

6. CHAIN MOTION AS A FUNCTION OF TEMPERATURE AND PRESSURE

All the parameters of the correlation time distributions, derived by fitting calculated spectra to the experimental spectra, are collected in Fig. 5. The indicated uncertainties in τ_0 and in Δ_σ are estimates of the ranges of these parameters for which satisfactory fits are obtained. Along all four isobars the results show the characteristic slowing-down of the dynamic process on approaching T_g from a higher temperature. At ambient pressure the time scale of the reorientation of the chain segments increases dramatically: from 1.9×10^{-8} s at 333 K to 30 s at 262 K, nine orders of magnitude in a temperature range of about 70 K. The width of the correlation time

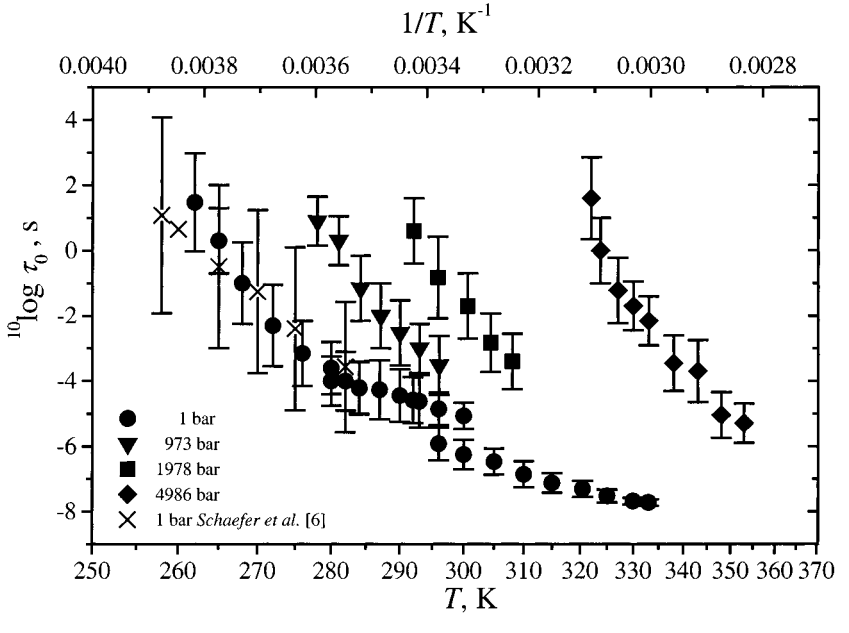

Fig. 5. Values of τ_0 (symbols) and Δ_σ (vertical bars) of the correlation time distribution as a function of pressure as obtained by comparing experimental and calculated ^{2}H-NMR spectra. Also included are the results of Schaefer et al. [6].

distribution increases from 0.2 to 3.0 decades in the same temperature range. The results obtained at ambient pressure are in good agreement with those in the temperature range 300 to 370 K obtained from 2D exchange ^{2}H NMR, reported in Ref. 6 (also shown in Fig. 5). They also nicely connect with those obtained from ^{13}C T_1 data [6, 8] in the temperature range from 300 up to 370 K, where the correlation time is about 2×10^{-10} s. At higher pressure the behavior, although measured in smaller intervals of temperature, appears to be very similar.

As is well known, in many polymer materials the slowing-down of the structural relaxation on approaching the temperature of the glass transition may be described by the empirical WLF relation [1, 2]. The form of this relation, in terms of an appropriate correlation time $\tau(T)$, is

$$\tau(T) = \tau(T_0) \exp[-c_1(T - T_0)/(T - T_0 + C_2)] \tag{4}$$

which, by substituting $T_0 = T_V + C_2$, is found to be equivalent to the Vogel–Fulcher–Tammann–Hesse (VFTH) relation [3–5],

$$\tau(T) = \tau_1 \exp[C_0/(T - T_V)] \tag{5}$$

with $C_0 = c_1 C_2$ and $\tau_1 = \tau(T_0) \exp(-c_1)$. In Eq. (4) T_0 is a reference temperature. In fact, it appears that the temperature variation of the value of τ_0, derived from our experiments can be described very well with the WLF equation. We use it, for convenience, as a basis for the representation of the whole data set. By introducing $C_1 = 2.303 c_1$ one obtains the form which is usually found in the polymer literature:

$$^{10}\log(\tau_0(T)/\tau_0(T_g(p))) = -C_1(p)(T - T_g(p))/(C_2(p) + (T - T_g(p))) \tag{6}$$

where T_0 is set equal to the glass-transition temperature $T_g(p)$.

We first used Eq. (6) to fit separately the data obtained at 1, 973, 1978, and 4986 bar. We reduce the number of free parameters by choosing for $\tau_0(T_g(p))$ a constant value along the glass transition line, for which we take its average value $10^{9.5}$ s as determined from separate fits to the data along isobars. The resulting WLF parameters $C_1(p)$ and $C_2(p)$ are collected in Table I. They show no clear pressure dependence. The dependence of τ_0 on $(T - T_g)$ does not change significantly at a pressure increase of up to 5 kbar; the dependence of τ_0 on T and p can be expressed simply as $\tau_0(T, p) = \tau_0(T - T_g(p))$.

7. CHAIN MOTION AS A FUNCTION OF DENSITY

Since for pressure values up to 5 kbar, the parameters C_1 and C_2 do not depend significantly on pressure, we can represent $\tau_0(T, p)$ by an

Table I. The Parameters $C_1(p)$ and $C_2(p)$ Resulting from Fitting the Temperature Dependence of τ_0 at Various Pressure Values with the WLF Equation

p (bar)	$T_g(p)$ (K)	$C_1(p)$	$C_2(p)$ (K)
1.2 ± 0.1	250 ± 2	21.1 ± 0.4	18.7 ± 1.1
973 ± 7	267 ± 1	19.7 ± 0.8	14.8 ± 1.5
1978 ± 14	279 ± 2	20.3 ± 0.9	16.7 ± 1.7
4986 ± 32	311 ± 1	20.2 ± 0.8	15.3 ± 1.6

empirical WLF function, with $\langle C_1 \rangle = 20.7$ and $\langle C_2 \rangle = 16.4$, the weighted averages of the values given in Table I:

$$^{10}\log(\tau_0(p, T)/10^{9.5}) = -20.7(T - T_g(p))/(16.4 + (T - T_g(p))) \tag{7}$$

For aPP pVT data are available [24–26] only for the melt. We have fitted the data of Ref. 26, obtained in the range 295 to 582 K, 0 to 2000 bar, for aPP with a weight-average molecular mass $M_w = 53400\ \mathrm{g \cdot mol^{-1}}$ with the Tait equation [27]:

$$\rho(p, T) = \rho(0, T)\{1 - D \ln[1 + p/(E_0 \exp(-E_1(T))]\}^{-1} \tag{8}$$

An accurate fit has been obtained by setting $\rho(0, T)^{-1} = a_0 + a_1 T + a_2 T^2$ with $a_0 = 42.3858\ \mathrm{cm^3 \cdot mol^{-1}}$, $a_1 = 1.50521 \times 10^{-2}\ \mathrm{cm^3 \cdot mol^{-1} \cdot K^{-1}}$, and $a_2 = 2.83996 \times 10^{-5}\ \mathrm{cm^3 \cdot mol^{-1} \cdot K^{-2}}$ and by taking $E_0 = 7256.3$ bar and $E_1 = 5.0897 \times 10^{-3}\ \mathrm{K^{-1}}$. The coefficient D is chosen to have the value 0.0894. We assume this equation of state also to be valid for our sample of aPP with molecular weight $M_v \approx 25{,}000\ \mathrm{g \cdot mol^{-1}}$ and use it for an extrapolation of the pVT data to the glass-transition temperature and to 5000 bar.

By substituting Eq. (2), expressing the pressure along the glass-transition line as a function of T_g, in the EOS, Eq. (9), we find that the density along the glass-transition line is represented by the quadratic function $\rho(p_g) = b_0 + b_1 p_g + b_2 p_g^2$ with $b_0 = 2.086 \times 10^{-2}\ \mathrm{mol \cdot cm^{-3}}$, $b_1 = 6.400 \times 10^{-7}\ \mathrm{mol \cdot cm^{-3} \cdot bar^{-1}}$, and $b_2 = -3.789 \times 10^{-11}\ \mathrm{mol \cdot cm^{-3} \cdot bar^{-2}}$. A pressure increase of 5000 bar results in an increase in the density at the glass transition of about 11%. A very similar increase in the density along the glass-transition line has been observed in other systems, for example, in poly(styrene) [28] ($\sim$2.1% per kbar) and poly(carbonate) [29] ($\sim$2.0% per kbar).

By introducing the equation of state, we obtain τ_0 as an empirical function of temperature and density. The resulting function is the surface

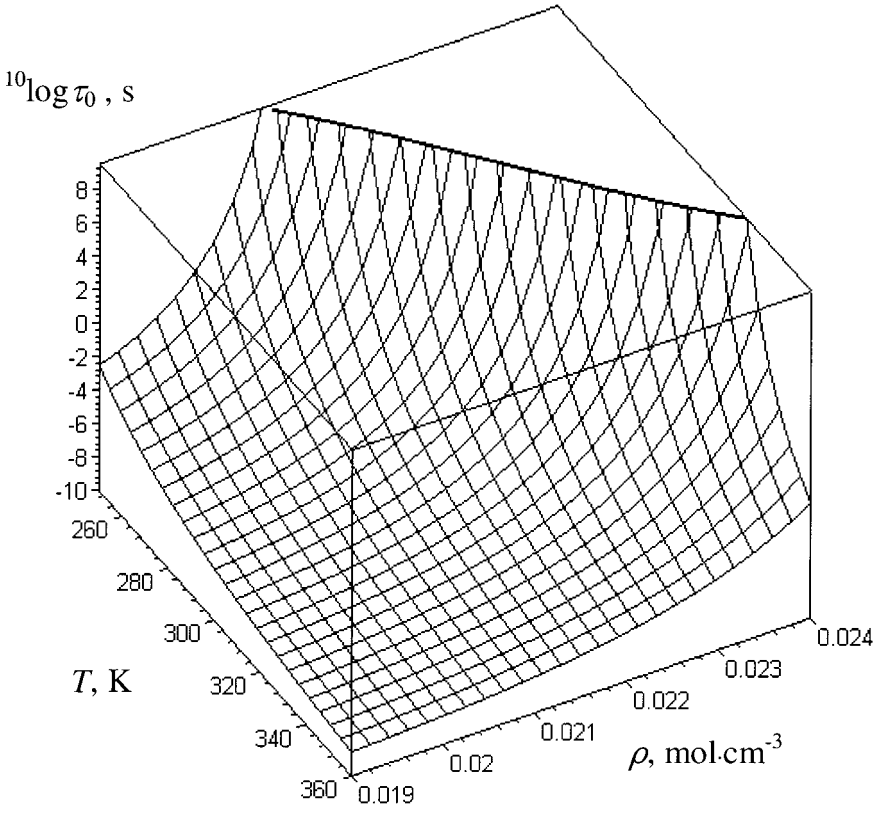

Fig. 6. WLF surface describing τ_0 as a function of temperature and density. The line at $^{10}\log \tau_0 = 9.5$ indicates the glass transition.

shown in Fig. 6. Its intersection at $^{10}\log \tau_0 = 9.5$ corresponds to the glass-transition line. The figure reveals that along the paths at constant temperature and at constant density, τ_0 shows the same steep increase, resulting in the arrest of the chain motion at the glass transition.

The behavior of τ_0 along isotherms and along isochores is very similar. Over a large temperature and density range τ_0 shows a WLF-like dependence on $T - T_g$ and on $\rho(T_g) - \rho(T)$, with parameters C_1', C_2' and C_1'', C_2'', respectively. Again setting the value of τ_0 at the glass transition to $10^{9.5}$, we obtain an excellent fit of the isochores with the WLF equation, resulting in the values $C_1' = 20.5$ and $C_2' = 19.8$ K. These values reflect a weaker temperature dependence of τ_0 along isochores, in comparison with that of τ_0 along isobars, for which the C_1 and C_2 values are shown in Table I. The isotherms are equally well fitted as a function of $\rho(T_g) - \rho(T)$ by a

WLF-like equation, with $C_1'' = 20.1$ and $C_2'' = 7.2 \times 10^{-4}$ mol · cm^{-3}. A fast WLF-type increase in τ_0 occurs both on an isochoric and on an isothermal path to the glass transition. The temperature dependence of τ_0 along isobars is slightly stronger than along isochores. This effect is small due to the fact that the density variation along an isobar is only small, so that the temperature change rather than the volume change has the dominant effect on τ_0.

As noted above, the dependence of τ_0 on temperature and pressure can be expressed simply as $\tau_0(T, p) = \tau_0(T - T_g(p))$, the lines $T - T_g(p) =$ constant are isochrones. Also at high pressures, the chain dynamics is completely determined by the same function of the temperature distance to the glass transition. This result is not self-evident, since the chain dynamics is strongly dependent on the density. As can be derived from the equation of state, the density along lines of constant $T - T_g(p)$ increases in approximately the same way as along the glass-transition line, namely, with about 11% over 5 kbar. The decrease in the rate of motion by an increase in density is just compensated by the increase caused by raising the temperature to the value required to remain at constant $T - T_g(p)$.

8. RELATION OF THE WLF PARAMETERS WITH THERMODYNAMIC QUANTITIES

A number of theories of the glass transition offer a physical basis for this relation, in particular, the statistical–mechanical theories of Adam and Gibbs [30–33] and of Parisi [34] and the "free volume" theory [2]. We compare our data with the results of the first theory, in which the polymer melt is considered to be composed of a number of subsystems, large enough to allow cooperative rearrangements of the chains into another configuration, without involving its environment. The subsystems are assumed to interact only weakly with the macroscopic system. It is shown that the overwhelming majority of rearrangements occur in the smallest regions, namely, those which permit a rearrangement at all. The probability for a rearrangement in the system can be expressed in the ratio s_c/S_c of the configurational entropy of the smallest cooperatively rearranging region to that of the macroscopic system and in the potential energy (per monomer segment) $\Delta\mu$ hindering the cooperative rearrangement. This probability is proportional to $\exp(-s_c \Delta\mu/(S_c kT))$. The configurational entropy of the smallest subsystem is $s_c = k \ln(\Omega)$, where Ω is the associated minimum number of possible configurations. On lowering the temperature, the smallest size of a cooperatively rearranging region will grow, until it comprises the complete macroscopic system at some temperature T_2, and the polymer melt is effectively frozen. The configurational entropy of the macroscopic system vanishes at this temperature T_2, which is somewhat below the

glass-transition temperature T_g determined in an experiment. With T_g chosen as the reference temperature, the WLF equation is derived with $C_1 = 2.303 \Delta\mu s_c/(k \Delta C_p T_g \ln(T_g/T_2))$ and $C_2 = T_g \ln(T_g/T_2)/(1 + \ln(T_g/T_2))$.

We compare our values for C_1 and C_2 from Table I with the results of the Adam and Gibbs theory and derive estimated values for T_2 and $\Delta\mu$. The discontinuity in the specific heat is known to be $\Delta C_p \approx 17.8$ $J \cdot mol^{-1} \cdot K^{-1}$ at ambient pressure [35]. In the range from ambient pressure to 5 kbar we have determined values for T_2 from 231 to 295 K. On average $T_g - T_2 \approx 17$ K, while, from comparison with experiments, Adam and Gibbs found $T_g - T_2 = 55 \pm 6$ K for a number of glass-forming liquids at ambient pressure. With $T_2 = 231$ K we derive $\Delta\mu s_c/k \approx 7.4$ $kJ \cdot mol^{-1}$ at ambient pressure. The rather high values for T_2 are related to the relative low values found for C_2 (when compared, for instance, with the values found in Ref. 30 for other substances). As the difference between T_g and T_2 is small, the result is quite sensitive to the factor $\ln(T_g/T_2)$ and, therefore, also to the values used for T_2. To make a somewhat more quantitative comparison we choose $\Omega = 2$, i.e., only two configurations are possible for the smallest cooperatively rearranging region, and find $\Delta\mu \approx 5$ $kJ \cdot mol^{-1}$, which is of the correct order of magnitude, namely, that of the potential energy barrier between a *trans* and a *gauche* conformation of an alkane chain [36]. Further analysis would require the knowledge of ΔC_p at high pressure. In principle, the Adam–Gibbs theory could be generalized to include the effect of density, but we did not attempt to do that.

Attempts to compare our data with the free volume theory [2] have led to conflicting results. Therefore, we concluded that a discussion of the effect of pressure on τ_0 in terms of the free volume theory is not very meaningful.

9. CONCLUSION

We studied the effect of high pressure on the motion of the main chain segments of aPP with different ^{2}H-NMR techniques in a large range of temperatures above its glass-transition temperature.

At and above the glass transition, small-angle motion of the chain segments, in which the chain C–^{2}H bonds participate, is superimposed on the much slower quasi-isotropic rotational diffusive motion, which is the result of collective behavior. This process causes the changes in the 1D and 2D ^{2}H-NMR spectra. Clearly, this process may be identified with the α-process observed in mechanical relaxation studies.

Our findings are consistent with the picture resulting from molecular dynamics simulations [37] of the local chain motion in amorphous polyethylene near the glass transition. The chain axis reorients much more

slowly than a vector attached perpendicular to the chain axis. Fast small-angle reorientation occurs within a restricted volume around the local main chain axis. In addition, chain segments take part in a slower quasi-isotropic rotational diffusion of the average local main chain axis, occurring as a result of the collective motion of its surroundings. On lowering the temperature, the time scales of the two processes become unrelated. Eventually, the collective rearrangement of the surroundings of the chain segments becomes too slow to be detected on the time scale of the experiment. This arrest of the motion is the glass transition. The fast, small-angle reorientation of the chain segments is not strongly affected by the glass transition.

From our experiments it follows that, on approaching the glass transition, the time scale of the collective motion of the main chain becomes longer very rapidly at decreasing temperatures. The temperature dependence of the logarithmic average correlation time is shown to be very well described by a WLF or VFTH function. The collective motion of the main chain is strongly dependent on pressure (or, rather, on density). The main result of this investigation is that it shows that, on an isothermal approach to the glass transition, the chain dynamics as a function of density also follows a Vogel–Fulcher-type law $\tau(\rho) \propto \exp[C(\rho_{VF} - \rho)^{-1}]$, which, in our opinion, is an important experimental finding. Although this result is obtained by the use of a partially extrapolated equation of state, the errors introduced in the density can only be minor.

ACKNOWLEDGMENTS

We would like to thank Prof. Dr. H. W. Spiess for his interest and for providing us with the sample material and the software for the analysis of the 2D data. This investigation is part of the research program of the Stichting voor Fundamenteel Onderzoek der Materie supported by the Nederlandse Organisatie voor Wetenschappelijk Onderzoek.

REFERENCES

1. M. L. Williams, R. F. Landel, and J. D. Ferry, *J. Am. Chem. Soc.* **77**:3701 (1955).
2. J. D. Ferry, *Viscoelastic Properties of Polymers* (John Wiley & Sons, New York, 1961).
3. H. Vogel, *Z. Phys.* **22**:645 (1921).
4. G. S. Fulcher, *J. Am. Ceram. Soc.* **8**:339, 789 (1925).
5. G. Tammann and W. Z. Hesse, *Z. Anorg. Allgem. Chem.* **156**:245 (1926).
6. D. Schaefer, H. W. Spiess, U. W. Suter, and W. W. Fleming, *Macromolecules* **23**:3431 (1990).
7. D. Schaefer and H. W. Spiess, *J. Chem. Phys.* **97**:7944 (1992).
8. A. Dekmezian, D. E. Axelson, J. J. Dechter, B. Bohra, and L. Mandelkern, *J. Polym. Sci. Polym. Phys. Ed.* **23**:367 (1985).

9. A. G. S. Hollander, Ph.D. thesis (University of Amsterdam, Amsterdam, 1998); copies are available on request.
10. J. H. Davis, K. R. Jeffrey, M. Bloom, M. I. Valic, and T. P. Higgs, *Chem. Phys. Lett.* **42**:390 (1976).
11. D. Schaefer, J. Leisen, and H. W. Spiess, *J. Mag. Res. A* **115**:60 (1995).
12. G. E. Pake, *J. Chem. Phys.* **16**:327 (1948).
13. K. Schmidt-Rohr and H. W. Spiess, *Multidimensional Solid-State NMR and Polymers* (Academic Press, London, 1994).
14. S. Kaufmann, S. Wefing, D. Schaefer, and H. W. Spiess, *J. Chem. Phys.* **93**:197 (1990).
15. C. Schmidt, B. Blümich, and H. W. Spiess, *J. Mag. Res.* **79**:269 (1988).
16. S. Wefing, S. Kaufmann, and H. W. Spiess, *J. Chem. Phys.* **89**:1234 (1988).
17. K. Schmidt-Rohr and H. W. Spiess, *Phys. Rev. Lett.* **66**:3020 (1991).
18. R. Kohlrausch, *Ann. Phys.* **12**:393 (1847).
19. G. Williams and D. C. Watts, *Trans. Faraday Soc.* **66**:80 (1970).
20. S. Wefing and H. W. Spiess, *J. Chem. Phys.* **89**:1219 (1988).
21. M. S. Greenfield, A. D. Ronemus, R. L. Vold, R. R. Vold, P. D. Ellis, and T. E. Raidy, *J. Mag. Res.* **72**:89 (1987).
22. H. Sillescu, *J. Chem. Phys.* **54**:2110 (1971).
23. A. Abragam, *The Principles of Nuclear Magnetism* (Clarendon Press, Oxford, 1961).
24. P. A. Rodgers, *J. Appl. Polym. Sci.* **48**:1061 (1993).
25. R. D. Maier, R. Thomann, J. Kressler, R. Muelhaupt, and B. Rudolf, *J. Polym. Sci. B Polym. Phys.* **35**:1135 (1997).
26. P. Zoller and D. J. Walsh, *Standard Pressure-Volume-Temperature Data for Polymers* (Technomic, Lancaster, PA, 1995).
27. P. G. Tait, *Phys. Chem.* **2**:1 (1888).
28. G. Rehage and H.-J. Oels, *High Temp. High Press.* **9**:545 (1977).
29. P. Zoller, *J. Polym. Sci. Polym. Phys.* **20**:1453 (1982).
30. G. Adam and J. H. Gibbs, *J. Chem. Phys.* **43**:139 (1965).
31. J. Jäckle, *Rep. Prog. Phys.* **49**:171 (1986).
32. J. H. Gibbs and E. A. DiMarzio, *J. Chem. Phys.* **28**:373 (1958).
33. E.A. DiMarzio and J. H. Gibbs, *J. Chem. Phys.* **28**:807 (1958).
34. G. Parisi, in *The Oscar Klein Centenary*, U. Lindström, ed. (World Scientific, Singapore, 1995).
35. E. Passaglia and H. K. Kevorkian, *J. Appl. Phys.* **34**:90 (1963).
36. P. J. Flory, *Statistical Mechanics of Chain Molecules* (Hansen, New York, 1969).
37. R.-J. Roe, *Advances in Polymer Science 116* (Springer-Verlag, Berlin/Heidelberg, 1994).